

Effect of Pressure on Pyrolysis of a Sub-bituminous Coal in an Entrained-Flow Reactor

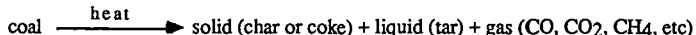
Mohammad Fatemi, Alan W. Scaroni, Chun Wai Lee and Robert G. Jenkins

The Pennsylvania State University
Combustion Laboratory
405 Academic Activities Building
University Park, PA 16802

Introduction

To help produce advances in gasification technologies it is necessary to generate data on the effect of coal properties and operating variables on the pyrolysis/gasification behavior of coals under conditions similar to those in advanced-concept gasifiers; usually a high temperature-high pressure environment for entrained coal particles. Since relatively little data are available on coal pyrolysis/gasification at elevated pressure, especially in entrained flow systems, the primary objective of this study was to provide information on the effect of pressure on product yield and composition during pyrolysis.

The thermal decomposition of coal produces solid char or coke plus liquid and gaseous volatile matter (1):



The char consists mainly of carbon along with small amounts of hydrogen, oxygen, nitrogen and sulfur as well as the ash produced from the mineral matter. Tars are vapors at the pyrolysis temperature and pressure. The quality and quantity of char, tar and gases produced during pyrolysis depend on coal type, temperature, heating rate, pressure, residence time and particle size (1).

Two general techniques have been used for coal pyrolysis studies (2): captive sample, where the coal is stationary or fixed during a run, and entrained-flow, where the coal is fed and products withdrawn continuously. Most data on pressure effects have been obtained using captive sample techniques (3-9). For example, Anthony et al. found a substantial reduction in weight loss with increasing pressure for the pyrolysis of a bituminous coal above 873 K (4). Suuberg et al. also reported a reduction in weight loss and tar yield with increasing pressure (7).

The entrained-flow technique, however, has been used more in recent years by researchers (10-16). Sundaram et al. examined the effect of pressure on pyrolysis of a sub-bituminous coal under various inert gas pressures (Ar, He and N₂) in an entrained-flow reactor (12). They reported that the tar yield increased with increasing pressure of helium, while it decreased with increasing pressure of argon. They also reported that the total carbon conversion went through a maximum before decreasing with increasing pressure. Serio et al., on the other hand, reported a reduction of about 25% in tar yield with increasing pressure for four different coals (13). A study similar to the one reported here on Montana Rosebud coal under the same pressure conditions but at higher temperatures and residence times has also been reported by Bissett (14).

Experimental

An entrained-flow reactor, which was capable of subjecting pulverized coal particles to temperatures and pressures of 1373°K and 1000 psig respectively for a range of particle residence times was used in this study. The reactor, which is equipped with a computerized data acquisition system for accurate monitoring of the experimental conditions, is shown schematically in Figure 1. Pulverized coal is injected into the furnace by entrainment in a cold gas stream (primary gas) as it passes through a semi-venturi. The coal laden gas flows through a water-cooled injector probe fixed at the top of the

furnace. A secondary gas stream which is preheated during its passage upward through an annular region surrounding the reactor tube enters the furnace near the tip of the injector probe. Char is collected by a water-cooled probe which can be adjusted over a range of distances from the bottom of the furnace. This gives the flexibility to change the pyrolysis residence time. Another method of changing residence times is to adjust the gas flow rates of the gases passing through the furnace.

Char is separated from the product stream in a filter vessel installed downstream of the collector probe. The particle-laden stream enters the cylindrically-shaped vessel tangentially and at a point midway up the vessel. The solid char falls into a sample vessel at the bottom of the cylinder, while much of the tar is trapped by a 20 μm stainless steel filter at the top of the vessel. The solid pyrolysis products and the material trapped by the filter both were extracted in a conventional Soxhlet apparatus using tetrahydrofuran (THF) as the solvent. The THF solubles, which are used to represent the tars produced during pyrolysis, were obtained by evaporating the solvent after extraction. The THF insolubles are used to represent the char yield.

Proximate analyses were performed on the chars using a Leco MAC-400 analyzer. Ultimate analyses were also performed on chars and tars using a Leco CHN-600 analyzer. Sulfur contents were measured by a Leco sulfur analyzer. The gas stream leaving the collector vessel is routed through an on-line Carle gas chromatograph which is capable of monitoring the following gases: H_2 , N_2 , O_2 , H_2S , CO , CO_2 , CH_4 , C_2H_2 , C_2H_4 , C_2H_6 , H_2O , SO_2 , and $\text{C}_3 + \text{C}_4$ hydrocarbons. An infrared gas analyzer is used to continuously monitor the carbon monoxide concentration in the outlet gas stream to determine when the reactor has reached steady-state operation. Gas composition measured by the GC is then determined for steady-state pyrolysis. The furnace is operated from a remote control panel and monitored by computer.

Samples of sized Montana Rosebud sub-bituminous coal, with mean particle size of 57 μm , were used in this study. Proximate and ultimate analyses of the raw coal are shown in Table 1. Pyrolysis experiments were performed at a temperature of 1189°K, applied N_2 pressures of 100-900 psig and residence times between 0.1 to 1.7 seconds. Coal particle residence times in the furnace were determined by using a computer flow model, which is a modified version of the one developed by Tsai for entrained-flow reactors operated at atmospheric pressure (17). We modified the flow model programs for use under our high-pressure entrained-flow reactor conditions.

Weight loss due to pyrolysis was calculated by using ash as a tracer. On a dry-ash-free basis, the governing equation is:

$$\Delta W = 100\% \left[1 - \frac{A_0(100 - A_1)}{A_1(100 - A_0)} \right]$$

where ΔW is the calculated weight loss on a daf basis, A_0 is the proximate ash content of the dry coal and A_1 is the proximate ash content of the dry char produced during pyrolysis. An assumption in this calculation is that mineral matter in the coal does not undergo transformations during the pyrolysis which would change the quantity of ash produced upon ashing the chars (15). Tar yields were calculated from the total amount of THF solubles collected, about 5-15%, and expressed as weight percent of coal (daf) fed into the reactor. Total gas yields were calculated from the difference between the weight loss and tar yield.

Results and Discussion

The effect of pressure on weight loss for pyrolysis at 1189°K, 0.3-1.0 seconds residence time and up to 900 psig applied N_2 pressure is shown in Figure 2. It is observed that at short residence times (0.3 and 0.5 seconds) increasing the pressure reduces the weight loss, but at a longer residence time (1.0 seconds) increasing the pressure increases the weight loss slightly after going through a minimum at 178 psig. The weight loss of the Montana Rosebud coal increased steadily with increasing residence time and reached a maximum at 1.0 seconds.

Figure 3 shows the effect of pressure on tar yield at 1189°K, 0.3-1.0 seconds residence time and up to 900 psig applied N₂ pressure. The tar yield increased significantly with pressure up to 178 psig for all residence times and, with the exception of short residence time (0.3 sec) tar, then continued to increase with increasing pressure but at a slower rate. The data are in agreement with those of Solomon et al., who reported similar tar yields for the Montana Rosebud coal at 1089°K and 0.47 seconds residence time (16). The data are also in general agreement with those of Sundaram et al. (12) who reported an increase in tar yield from a sub-bituminous coal with increasing pressure of helium.

Yields and composition of gaseous products are shown in Figures 4 and 5, respectively. Comparison of Figures 2, 3 and 4 indicate that the trend for total gas yield is consistent with the effect of pressure on weight loss and tar yield. The total gas yield drops as the pressure increases from 100 to 178 psig then increases slightly with further increase in pressure. This is also in a good agreement with the data of Solomon et al. At short residence time (0.3 seconds) CO and CO₂ yields increased significantly with increasing N₂ pressure while the CH₄ yield decreased. Reduction in CH₄ yield with increasing pressure has been reported by Serio et al. (13) In the experiments carried out at residence times higher than 0.3 seconds CO concentrations were higher than CO₂, and the concentration of CH₄ was higher than that of C₂H₄ which, in turn, was higher than C₂H₆. This is in good agreement with the data of Sundaram et al. (12) but agrees with that of Serio et al. (13) only for the CH₄, C₂H₄ and C₂H₆ hydrocarbon gases.

The effect of pressure on the C/H ratio of the tar and char produced from pyrolysis is shown graphically in Figure 6 and 7, respectively. It can be seen in Figure 6 that the C/H ratio of the tars remains relatively constant except at short residence times where there is a significant drop in the C/H ratio at 178 psig. Figure 7, on the other hand, shows that the C/H ratio of the char decreases significantly as pressure increases. At short residence times the C/H ratio of the char drops from over 1.8 at 100 psig to below 1.4 at 178 psig then remains relatively constant. At the longer residence time the C/H ratio decreases gradually from over 2.2 at 100 psig to 1.8 at 900 psig N₂ pressure.

Conclusions

Pyrolysis of a Montana Rosebud subbituminous coal in a high pressure entrained flow reactor revealed the following:

1. Based on the weight loss, tar and gas yield, and C/H ratio of the tar and char, it appears that a significant change in pyrolysis behavior occurs at a pressure between 100 and 178 psig.
2. Weight loss and gas yield decrease with increasing pressure up to about 200 psig, and above this pressure there is no significant effect.
3. Tar yield is most affected by the pressure, increasing significantly with increasing pressure up to 200 psig.
4. The maximum tar yield was observed at a low residence time (0.3 seconds) and 178 psig applied N₂ pressure.
5. The CH₄ and C₂H₆ yields decreased significantly with increasing pressure, with C₂H₆ diminishing above 300 psig pressure for a residence time of 1.0 second.

References

1. Normand, M. L., "Heterogeneous Kinetics of Coal Char Gasification and Combustion," *Prog. Energy Combust. Sci.*, Vol. 4, 1978, pp. 221-270. (Pergamon Press Ltd., Great Britain).
2. Anthony, D. B. and Howard, J. B., *A.I.Ch. E. J.*, Vol. 22, 1976, pp. 625-656.
3. Anthony, D. B., Howard, J. B., Hottel, H. C. and Meissner, H. P., 15th Symposium (Int.) on Combustion, *The Combustion Institute*, Pittsburgh, PA, 1975, pp. 1303-1317.

4. Anthony, D. B., Howard, J. B., Hottel, H. C. and Meissner, H. P., *Fuel*, Vol. 55, 1976, pp. 121-128.
5. Solomon, P. R. and Colket, M. B., 17th Symposium (Int.) on Combustion, *The Combustion Institute*, Pittsburgh, PA 1979, pp. 131-143.
6. Suuberg, E. M., Peters, W. A. and Howard, J. B., *Ind. Eng. Chem. Process Des. Devel.*, Vol. 17, 1978, pp. 37-46.
7. Suuberg, E. M., Peters, W. A. and Howard, J. B., *Fuel*, Vol. 59, 1980, pp. 405-412.
8. Niksa, S., Russel, W. B., Saville, D. A., 19th Symposium (Int.) on Combustion, *The Combustion Institute*, Pittsburgh, PA, 1982, pp. 1151-1158.
9. Arendt, P. and van Heek, K., *Fuel*, Vol. 60, 1981, pp. 779-787.
10. Kobayashi, H., Howard, J. B. and Sarofim, A. F., 16th Symposium (Int.) on Combustion, *The Combustion Institute*, Pittsburgh, PA, 1977, pp. 411-425.
11. Solomon, P. R., Hamblen, D. G., Goetz, G. J. and Nsakala, N. Y., *Preprints. Div. Fuel Chem.*, Am. Chem. Soc., Vol. 26, No. 3, 1981, pp. 6-17.
12. Sundaram, M. S., Steinberg, M., and Fallon, P. T., *Preprints, Div. Fuel Chem.*, Am. Chem. Soc., Vol. 28, No. 5, 1983, pp. 106-129.
13. Serio, M. P., Solomon, P. R. and Heninger, S. G., *Preprints, Div. Fuel Chem.*, Am. Chem. Soc., Vol. 31, No. 3, 1986, pp. 210-221.
14. Bissett, L. A., *Preprints, Div. Fuel Chem.*, Am. Chem. Soc., Vol 31, No. 3, 1986, pp. 222-229.
15. Jenkins, R. G. and Scaroni, A. W., Proceedings of the Sixth Annual Gasification Contractors Meeting, DOE/METC -86/6043, 1986, pp. 171-181.
16. Solomon, P. R., Serio, M. A. and Hamblen, D. G., Proceedings of the Sixth Annual Gasification Contractors Meeting, DOE/METC-86/60 43, 1986, pp. 182-191.
17. Tsai, C. N., "An Experimental Investigation of the Initial Stages of Pulverized Coal Combustion," Ph.D. Thesis, The Pennsylvania State University, 1985.

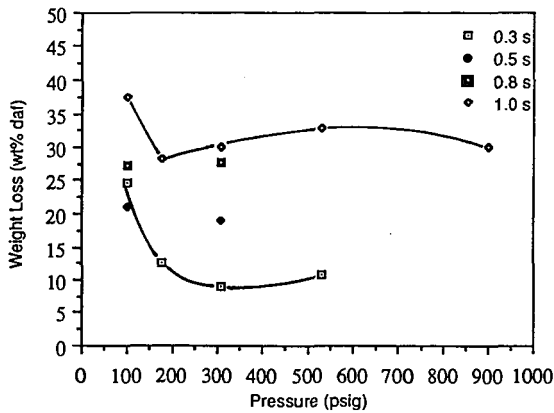


Figure 2. Effect of Pressure on Pyrolysis Weight Loss from Montana Rosebud Coal at 1189 K

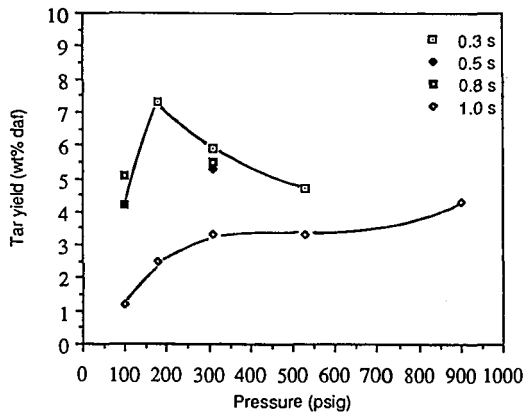


Figure 3. Effect of Pressure on Pyrolysis Tar Yield from Montana Rosebud Coal at 1189 K

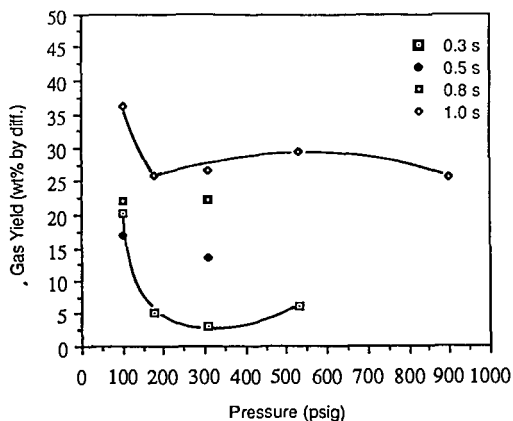


Figure 4. Effect of Pressure on Pyrolysis Gas Yield from Montana Rosebud Coal at 1189 K

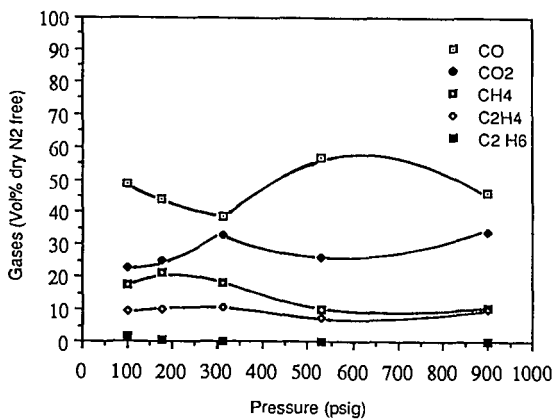


Figure 5. Effect of Pressure on Pyrolysis Gas Composition from Montana Rosebud Coal at 1189 K and 1.0 s

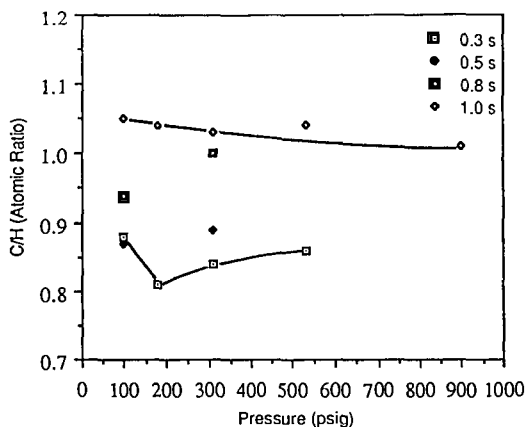


Figure 6. Effect of Pressure on C/H Ratio of Tar from Pyrolysis of Montana Rosebud Coal at 1189 K

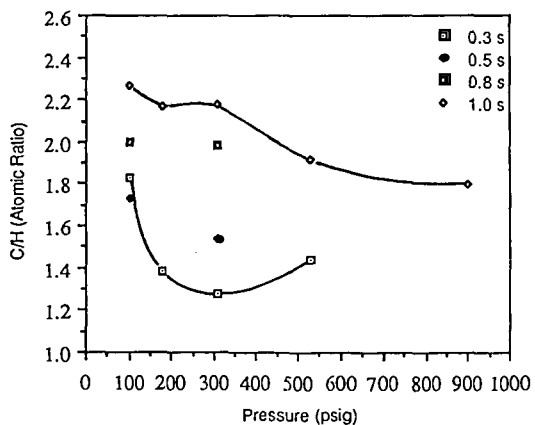


Figure 7. Effect of Pressure on C/H Ratio of Char from Pyrolysis of Montana Rosebud Coal at 1189 K

MODELING OF COAL PYROLYSIS UNDER THE CONDITIONS OF AN ENTRAINED PHASE REACTOR

W. Wanzl, P. Kaßler, K.H. van Heek, H. Jüntgen
Bergbau-Forschung GmbH, D-4300 Essen 13, West Germany

INTRODUCTION

Experimental laboratory work has shown that yield and quality of liquid products from coal pyrolysis can be controlled and optimized to a certain extent by suitable coaction of the primary thermal coal decomposition reactions and the secondary cracking or hydrocracking of the volatiles. The results indicate that favorable process conditions are provided in an entrained phase transport reactor which enables high heating rates for fast primary coal pyrolysis together with optimum residence time of the volatiles for secondary cracking and hydrocracking in the heated reactor zone. From that point of view the question arises how thermal coal decomposition can be described at high heating rates and whether transport limiting processes are involved in the overall reaction step. Especially for reactor design it is necessary to clarify to what extent experimental kinetic data gained at low heating rates can be applied to heating conditions like in a fluidized bed or in an entrained phase reactor.

KINETIC EXPERIMENTS

Low Heating Rates - Thermobalance Experiments

For experimental investigations of the influence of heating rate on the kinetics of coal pyrolysis three different types of equipment have been used as shown in Fig. 1. In previous work at low heating rates the course of product formation - total weight loss, tar, and gas - depending on temperature was measured in non-isothermal experiments in a thermobalance /1/. The low heating rate of some K/min in the thermobalance allows, beside the recording of the decrease in mass of the coal sample, a continuous analysis of the product gases (including detection of H₂O) and, by difference between total mass loss and total gas formation, the calculation of tar formation.

The mass loss curve as well as the curves for the different gaseous components show a certain structure which indicates that the volatiles are liberated in several single reactions for each component. The reactions can in a first order be regarded as a set of independent parallel reactions. This model of non-isothermal reaction kinetics allows a mathematical description of product formation. With the model equations the measured curves can be described by fitting activation energy E and frequency factor k_0 .

High Heating Rates - Grid Heater Experiments

The verification of the measured kinetic data at high heating rates has been carried out in experiments with a grid heater and with a Curie-point pyrolysis equipment. Schwandtner /2/ used a grid heater in the vacuum chamber of a time of flight mass spectrometer and applied heating rates up to 3000 K/s. The fast response signal of the mass spectrometer enabled kinetic measurements at high heating rates. According to theoretical calculations with the equations describing the non-isothermal reaction kinetics Schwandtner found a significant influence of the heating rate on the gas formation curves, which were shifted towards higher temperatures, respectively towards later times. But additionally, the gas release was shifted with rising particle

size as shown in Fig. 2. For coal grains exceeding 0.4 mm in diameter furthermore a tailing at the end can be noticed. With further enlargement of the grain size up to 1 mm and more the gas formation rate becomes independent of time. This means a reaction order of 0, which expresses the increasing influence of heat conductivity at these experimental conditions. This effect can be explained by the assumption that the heat transfer into the grain limites at certain heating rate and particle size the overall pyrolysis reaction. By a simple calculation of the temperature profile in the coal particle and integration of the total gas formation in the particle on the basis of a shell model the measured curves can be fitted as shown in Fig. 2.

High Heating Rates - Curie-Point Experiments

By using a different heating technique similar investigations were carried out with a pressurized Curie-point equipment which allows high heating rates above 10,000 K/sec and by that nearly isothermal pyrolysis experiments /3/. The method for measuring the critical particle diameter above which the transition from chemical reaction control to transport rate control occurs, involves measuring the yield of pyrolysis products, mainly the tar, at incomplete coal decomposition reaction. At a given heating rate and pressure, mass loss is independent of particle diameter at low particle size. By increasing particle size a distinct drop in the mass loss is noted as shown in Fig. 3, indicating that mass and/or heat transfer effects inhibit the escape of the volatiles from the particle. The critical particle diameter can, therefore, be determined by the change in the trend of mass loss versus particle size and finally plotted as function of heating rate (Fig.4).

HEAT TRANSFER CALCULATIONS

In order to achieve a more precise separation between the experimentally measured mass and enthalpy transport effects and their relevance for the measurement of kinetic pyrolysis data, model calculations were performed. The model assumes a spherical coal grain with its surface heated time dependently. It includes reaction enthalpies uniformly distributed in the coal particle. Intraparticle temperature profiles are then calculated using boundary conditions specific to the different heating methods in each apparatus.

The result of a calculation reproducing the conditions in the Curie-point measurements at a heating rate of 6.000 K/s for grain sizes at and above the critical radius (0.1 mm and 2 mm respectively) is shown in Fig. 5. The temperature profiles show quite clearly the existence of the measured critical diameters being in a first approximation a result of heat conduction within the coal. These radii are the limit up to which the heating rate can cause intra particle temperature gradients. The thermobalance uses a heating rate of 3 K/s, slow enough to prevent temperature gradients within the particle. With grain sizes below 0.1 mm also the pyrolysis yields of the Curie-point apparatus at heating rates up to 10,000 K/s may be evaluated without having to account for non-isothermal coal grains (Fig. 6).

As a consequence, looking at temperature profiles in a grain with the surface heated up instantaneously, as an upper limit for the conditions in an entrained phase reactor, internal temperature profiles die out after some ten milliseconds. These are time increments of the order of magnitude needed to reach thermal equilibrium between gas and coal within the very beginning of the reaction tube. The description of reaction kinetics in such a reactor type should therefore be possible on the basis of experimental data gained with the thermobalance and the curie point apparatus.

REFERENCES

- 1) Schwandtner, D.; Entgasung von Steinkohlen bei Aufheizgeschwindigkeiten oberhalb 10^3 grad/min, Thesis, Aachen. 1971
- 2) Wagner, R., W.Wanzl, K.-H. van Heek.: Fuel 64 (1985) 571.
- 3) Bunthoff, D., W.Wanzl, K.-H. van Heek, H. Jüntgen: Erdöl und Kohle Vol. 36 (1983) 326

ACKNOLEGDEMENT

The work was carried out within the frame of the IEA-Pyrolysis project (sponsored by the governments of Germany, Sweden, and United Kingdom) and within the project Anwendungsorientierte Grundlagenforschung (sponsored by the Bundesminister für Forschung und Technologie, Germany).

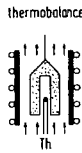
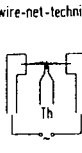
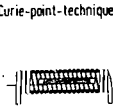
	thermobalance	wire-net-technique	Curie-point-technique
apparatus			
sample size mg	1,500	10	5
heating rate K/s	0.05	200-1,500	10,000
final temperature °C	1,000	1,000	adjustable
			isothermal experiments
results	kinetics of product formation E, k_0, n, V_0 for H_2, CO_x, C_xH_y , BTX and tar product yield	kinetics of particle swelling from high speed camera studies	kinetics of product formation E, k_0, n, V_0 for H_2, CO_x, C_xH_y , BTX and tar product yield

Fig. 1: Laboratory Equipment for Pyrolysis Experiments

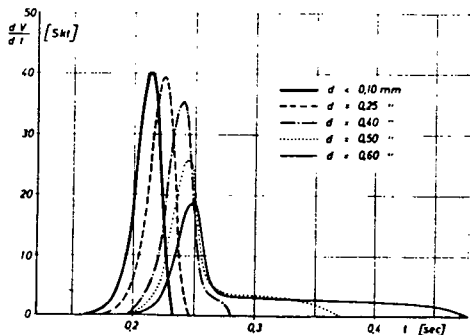
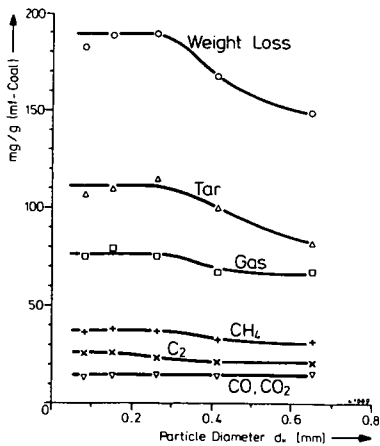


Fig. 2: Calculated Devolatilization Curves ($E = 240$ kJ/mol, $k_0 = 10^{11}$ min⁻¹)



Coal: GFK Westerholt
 Gas Atmosphere: N₂
 Pressure: p = 15 MPa
 Final Pyrolysis Temperature: T_f = 800°C
 Heating Rate: m = 9000 K/s
 Pyrolysis Time: t = 1.0 s

Fig. 3: Influence of Particle Size at High Heating Rates

Gasflammkohle Westerholt
pyrolysis temperature 800°C

- 0.01 MPa N₂
- 5 and 15 MPa N₂
- 10 and 15 MPa H₂

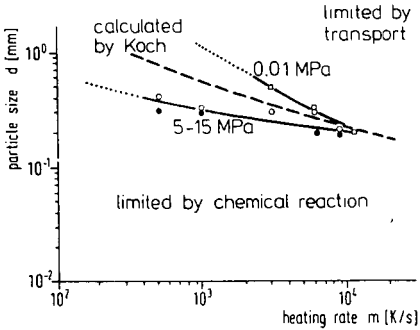


Fig. 4: Reaction Rate Limiting Step Depending on Heating Rate and Pressure

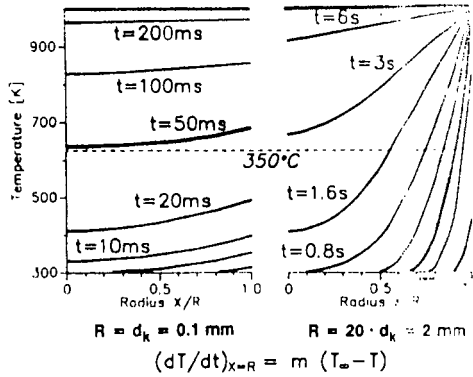


Fig. 5: Internal Profiles at and above Critical Radius d_k

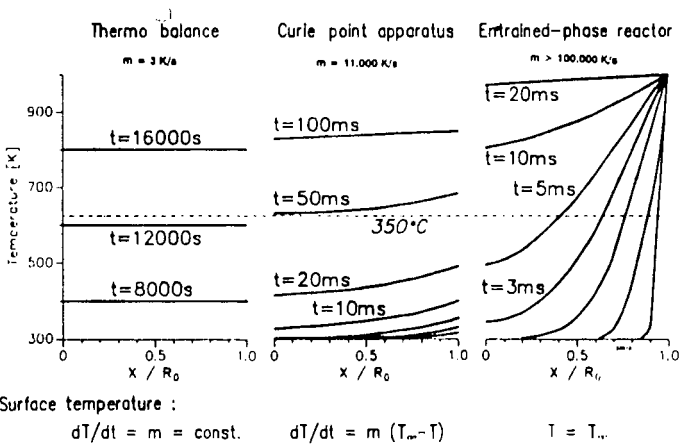


Fig. 6: Intra - Particle Temperature Gradients at Different Experimental Conditions

EFFECT OF HEAT TRANSFER ON TAR AND LIGHT GASES FROM COAL PYROLYSIS

J. D. Freihaut, W. M. Proscia, D. J. Seery

United Technologies Research Center
East Hartford, CT 06108

INTRODUCTION

Recent evidence has demonstrated that the products of coal pyrolysis vary with the conditions of heating. Both the reactivity of the char and the chemical composition of the evolved species vary with thermal flux during pyrolysis. Because of the inherent complexity of coal, it is difficult to uncouple the actual heat transfer process and the effects of variations in individual parameters in most pyrolysis experimental designs. Typical ranges of heat transfer rates available in a number of devolatilization reactor systems are indicated in Fig. 1. A particular reactor system may have additional constraints imposed by the nature of the heat flux source or transfer media - acceptable particle size of the parent coal, ambient pressure in which devolatilization can be performed, spectral distribution of a radiant source, residence time in the heat transfer field, etc. Some practical size constraints of wire grid and entrained flow reactor systems are noted in Figure 1.

This report presents the results of a study of coal pyrolysis in three different reactors covering a wide range of heating conditions. The specific purpose of the investigation was to determine if the rate of heat delivery to a high volatile bituminous coal during the tar formation and evolution phase has a significant effect on the tar yields and molecular weight distribution for a high volatile bituminous coal. From the point of view of understanding coal devolatilization and the development of fundamental kinetic models, the investigation is geared to determining whether the same tar formation and evolution processes are occurring in widely different regimes of heat transfer rate and modes of heat transfer. The heavy hydrocarbons yields and chemical characteristics provide a type of observable monitor, to generate a microscopic model of the devolatilization/pyrolysis process.

EXPERIMENTAL

Reactor Characterization

The influence of transport on coal devolatilization necessitates the characterization of reactor heat transfer properties in detail. Figure 1 displays the power density regimes required for a given heating rate of inert, spherical particles having thermal capacities equivalent to coal. Also shown are the range of power density capabilities of the heated grid and flash lamp reactors employed in this investigation and the corresponding regimes for entrained flow reactors. The heated grid system employed in this investigation generates power densities of 1-6 watts/cm² at grid temperatures between 600°K and 1200°K. The flash lamp system generates power densities, in the form of transient irradiance levels. Time averaged levels from 200 watts/cm² to greater than 700 watts/cm² were employed. Entrained flow reactors generally operate in the 10-100 watts/cm² regime. Final particle

temperatures of 1000°K or greater can be obtained in each system, but for significantly different transient times.

UTRC Heated Grid (HG)

The heated grid experiments are conducted by imposing a controlled voltage across a folded No. 325 mesh stainless steel screen. The screens are prefired, then loaded with 20-30 mg of coal by evenly distributing the coal between the folds of the screen. Simultaneous, real time measurements of applied voltage across the screen, current flow, and temperature of the screen are made by a rapid data acquisition system. The grid, char and tar are quenched by impingement of high velocity helium jets on the grid at the end of the heating program. The light gases evolved are measured by a FT-IR gas analysis system attached directly to the heated grid cell. Details of the UTRC heated grid apparatus have been given previously (Ref. 1, 2). The power density fields in vacuum conditions consist mainly of irradiance, whereas in the presence of ambient gases there can be significant gas conduction depending on the thermal conductivity of the gas. The power density fields were determined by synchronously measuring delivered current and voltage while measuring the temperature of the screen at pseudo steady-state conditions, and normalizing with respect to screen surface area. Depending on the heat transfer and heat capacity properties of the sample relative to the screen and ambient gas, the sample can couple to the local power density field. Such coupling has been demonstrated to change the observed temperature trajectory of the screen relative to an unloaded screen area (Ref. 1, 2). The main element of interest is the magnitude of the power density levels established by the heated grid system in the 600°K to 1000°K screen temperature regime, the temperatures of tar formation and evolution in such heating systems (Refs. 3, 4, 5).

UTRC Flash Lamp (FL)

Details of the flash lamp reactor have been given previously (Ref. 6). Under the range of capacitor voltage levels used in this investigation and with the particular match of lamp characteristics and driving circuit parameters the shape of the pulse did not vary significantly. The magnitude of the irradiance level delivered to the inside of the reactor was controlled by varying the neutral density filter and/or the capacitor bank voltage levels. The real time irradiance levels of the flash pulse were monitored by fast response pyroelectric detectors. The detectors employed were calibrated with NBS irradiance standard lamps and a NBS traceable radiometer system used in conjunction with a chopped Argon ion laser. Pyroelectric detectors have a nearly constant response to wavelength from the UV to IR spectral regimes. Because of the possibility of inducing photochemical reactions with the UV component of the flash pulse, the reactors employed were pyrex, as were the neutral density filters. The delivered radiation is characterized by wavelengths ranging from 0.4 to 2.0 microns with peak intensities between 0.8 and 1.1 microns.

Entrained Flow Reactor (EF)

In the entrained flow reactor, coal is entrained in a primary gas and injected into a hot wall furnace, through which a preheated secondary gas is flowing whose temperature is matched with the wall. Entrained coal/char particles flow in a pencil-like stream down the center of the furnace tube and

are collected by a water cooled probe. Figures 2, 3 and 4 display the overall reactor design, aerosol-char separation device and the aerosol and char separation trains. Approximately 75% of the total reactor flow is diverted to the aerosol train. Both the cyclone (char) train and impactor (aerosol) train are followed by final filters. These filters consist of porous metal disks to ease in removal of tar species. Approximately 90% of the tar mass appears to collect on the final filters, with some deposition on stages 7 and 8 of the impactor train. SEM analysis of the impactor and cyclone stages as well as the final filters reveal the phase separator extracts particulates and aerosols less than 2 microns from the particulate flow at 75% gas flow removal. Tar material deposited on the final filter substrates consists almost entirely of condensed heavy hydrocarbons having no particulate boundary structure. Particulate material is efficiently removed by the impactor and cyclone stages.

Because the coals were initially size separated by aerodynamic means, it was originally thought that the size specific ASTM ash could be used as the basis for calculating mass fraction loss via the ash tracer technique. However, using this value gave negative weight loss results for the low wall temperature runs. Inspection of the gas analysis system data and the filter stages of the cyclone and impactor trains indicated substantial devolatilization was occurring. It became apparent that the feed system was not delivering coal particles having the same average ash content as measured for the gross sample for this particular size cut. Consequently, the reactor system was operated in the cold wall, cold flow mode with the delivered coal particles collected in stage 0 of the cyclone separator considered as representative of the actually delivered samples. It was noted that immeasurably small samples of fines were deposited in the impactor train or subsequent stages of the collection system.

Tar Sampling and Handling

Tar yields in the heated grid reactor are determined by weighing the condensable material deposited on the inside of the reactor walls and filters placed between the reactor and FT-IR gas cell. Tar yields in the flash lamp reactor are defined as the THF soluble portion of the condensibles found inside the reactor and on the filters placed between the reactor and FT-IR gas cell. These tars may contain material extracted from char particles in addition to "desorbed" (vaporized molecules, ejected molecular clusters and colloidal fragments) species evolved in the flash heating process. Relative molecular weight distributions of tars were determined with the THF soluble (room temperature, ten minute ultrasonic bath) portion of the evolved species. Entrained flow reactor tars were defined as the THF soluble portion of the material removed from the filtering system. All samples were passed through a 0.5 micron filter before injection into the SEC system. The details of the SEC have been given previously (Ref. 7).

RESULTS AND DISCUSSION

Tar yields and relative molecular weight distributions were obtained for PSOC1451. The elemental analysis for the mesh and aerodynamically separated coal samples are given in Table Ia. Table Ib lists the elemental compositions observed for the 20 - 30 micron cut of the parent coal PSOC 1451 D sample, the delivered particles captured in stage 0 of the cyclone collector, and the residual particles remaining in the feeder bed after several runs. Obviously,

the feed system delivers 20 - 30 micron particles having lower average mineral densities than that observed for the gross parent sample. The residual particles, that is, the particles left in the feeder bed have higher average mineral densities than the gross parent sample. Despite the fact that the size separation system and the feeder system both employ aerodynamic principles, segregation does occur in the reactor feed process. As a result it was deemed necessary to perform cold flow runs with each sample to generate baseline ash data for determining mass reaction yields by ash tracer calculations. Results for tar yields, number average (Mn), and weight average (Mw) molecular weights are summarized in Table II. The data have been arranged in order of increasing net power density. The incident power density has been estimated from reactor property measurements indicated above and heat balance calculations assuming coal particles are spherical, with emissivity and absorptivity of 0.9, and heat capacity of 0.3 cal/gm-C. The particle sizes listed are an arithmetic average diameter of the high and low cutoff of the mesh range. The entrained flow tar yields are estimates based on one atmosphere runs performed in the flash lamp and heated grid reactor where particles were heated to the same final temperatures.

The limits of the molecular weight distributions range from 100-3500 for the heated grid and entrained flow tars, and from 100-5000 for the flash lamp tars. Previous investigators have obtained similar results for average molecular weights and for the range of the MWD's of various coal tars, and coal extracts (see Table III).

Pressure Effect in a Particular Reactor

Heated grid and flash lamp experiments were conducted at atmospheric and low pressures. The entrained flow reactor was operated at one atmosphere only. Comparisons of heated grid and flash lamp data given above (Table II) reveal a highly coupled dependency between mass and heat transfer parameters in determining molecular weight characteristics of the evolved tars. Larger MWD moments are obtained with the heated grid apparatus under low pressure conditions relative to atmospheric pressure for a given power program input (Fig. 5). The low pressure tars obtained in this apparatus have a significantly larger fraction of high MW species than the corresponding atmospheric pressure tars. Tar yields are reduced by 30% or more, depending on specific conditions, while molecular weight moments are reduced. These results are consistent with the results of Unger and Suuberg (Ref. 8) and others (Ref. 9, 10).

The same MWD pattern emerges at the lowest power density inputs employed with the flash lamp apparatus. That is, the low pressure tars have significantly higher molecular weight moments than the corresponding tars formed in one atmosphere of helium or argon (Fig. 5). However, at the next highest irradiance level (285 w/cm²) the tars formed in one atmosphere of helium have larger moments than the corresponding low pressure conditions. These results can be understood relative to the variation in heat transfer conditions. Particles subject to a radiant pulse in low pressure conditions can only cool by an ablative process whereas particles radiantly heated in the presence of an ambient gas are cooled by conduction across a boundary layer as the particle temperature rises. In low pressure conditions the tars formed within the heating particle become hot enough to undergo some secondary cracking reactions in the evolution process. Depending on its thermal conductivity, the moderating influence of the ambient gas can be appreciable,

resulting in a lowering of the net power density delivered to the particles. Consequently, the lowest irradiance level employed was not sufficient to heat the 50 micron particles, in the presence of helium, to desorb more than 5 to 10% of the coal mass as tars. In vacuum conditions, on the other hand, the observed tar yield was ~23% for the lowest irradiance level. In one atmosphere of argon the yield was ~19% with MWD moments similar but somewhat lower than the corresponding vacuum run. The results also indicate that the change in irradiance level from an average level of 225 w/cm² to 285 w/cm² in low pressure conditions results in thermal cracking reactions of the tars as they are evolving from the correspondingly hotter particles. Light gas - CH₄, CO, C₂H₂, C₂H₄, HCN-yields associated with such high temperature reactions of tars are also increased. Although increases in CH₄ and CO are observed in the heated grid gas yields when the tar evolution process is performed in pressure as opposed to vacuum, significant changes in C₂H₂ and HCN are not observed for this coal type with a change in ambient pressure alone.

Variation in Molecular Weight Distributions with Power Density Level

The influence of power density on tar yields and MWD's was explored by utilizing the multi-reactor approach discussed previously. The effect of large differences in power density is explored by comparing results from different reactors for a particular ambient gas environment (Figure 6). The heated grid tars, which were devolatilized at the lowest incident power fields are observed to have lower number average and weight average molecular weights than the flash lamp tars, devolatilized at the highest power densities. The main mode of energy transfer is radiation in these reactors when operated in low pressure conditions, although the wavelength distribution of the radiation is shifted to the visible and near IR for the flash lamp relative to the heated grid. The molecular weight moments of the entrained flow reactor tars vary substantially with residence time. In order to compare results to the other reactors, the shortest residence time tars should be examined since these presumably will have experienced the smallest degree of gas-phase secondary reactions. The tars produced in the 900°C, 40 msec residence time conditions have slightly lower molecular weights than the atmospheric pressure heated grid tars while the 1000°C, 40 msec tars show similar moment characteristics. In both cases the initial tars (low residence time) show molecular weight moments less than the vacuum tars formed in the heated grid. Relative to the flash lamp tars generated in either vacuum or pressure conditions the EF reactor tars have lower moment and distribution characteristics.

Devolatilization Modeling and Coal Structure

For a given set of heat transfer conditions and particle size, it can be difficult to distinguish between mass and heat transfer effects on volatiles product distributions and characteristics (Ref. 11). Both phenomena can appear to effect any one observable similarly by introducing intraparticle or extra-particle (particle-gas boundary layer or entrainment stream) secondary reactions in evolving tar species. Lumped parameter measurements - tar yield, char yield, gas yield, weight loss - are not informative and can even be misleading for a microscopic understanding of coal devolatilization. Kinetic comparisons based on one yield characteristic or product type grossly oversimplify the complexity of the process and can be even more misleading. The results reported in this investigation indicate that detailed

characteristics of tar species generated under one set of reactor conditions can give more insight into the devolatilization process, but only if careful consideration of reactor conditions are included and detailed comparisons are made to results obtained with other reactors on the same analytical bases. A combination of tar characteristics and light gas yields and composition for a wide range of reactor conditions are necessary before a comprehensive understanding of coal devolatilization can be established.

The significant change in relative MWD's of desorbed tars with heat transfer rate in low pressure conditions strongly implies a wide distribution of bonding types, ranging from predominantly physical association to covalent bonding, among a wide distribution of organic structure sizes, molecular to colloidal. The "tar" characteristics depend on the rate (power density field) at which thermal energy is delivered to the organic matrix, the mode of energy delivery and mass transport conditions. Such behavior is not unlike that exhibited by large, thermally labile organic molecules which are observed to desorb from a given substrate intact, via pyrolysis fragmentation, or in both forms, depending on the specific mass and heat transfer conditions and the nature of the molecular interactions between the adsorbed molecules and substrate (Ref. 12-19). From a devolatilization perspective high volatile bituminous coals behave as if they contain a wide range of organic structures, molecular and colloidal, attached to a polymeric-like substrate by a variety of physical and chemical bonding types. The presence of specific fractions of physically and chemically bonded species has been postulated to interpret the plastic behavior and generation of intraparticle pyridine extratables during the rapid heating of an Appalachian provide high volatile bituminous coal (4, 40). The size characteristics of the desorbed species varies depending on whether pyrolysis fragmentation or desorption of relatively large species is emphasized by the heating conditions employed in devolatilization as well as mass transport related parameters.

Acknowledgements

The authors are grateful to Dr. D. Maloney for providing tar samples for comparisons. D. Santos and G. Wagner provided critical technical assistance in carrying out this investigation. Partial funding was provided by the Department of Energy under Contract DE-AC22-84PC70768.

TABLE Ia

PSOC 1451 (HVA BIT - Appalachian Province)
Elemental Composition

Mesh <d>	-270+325 49	-100+140 127	-50+70 254	-25+35 604	-20+25 774
%DAF					
C	82.38(0.47)*	82.26(0.36)	82.28(0.36)	80.66(2.80)	78.40(4.87)
H	5.44(0.03)	5.54(0.03)	5.58(0.02)	5.71(0.28)	5.69(0.20)
N	1.60(0.03)	1.62(0.02)	1.63(0.01)	1.56(0.08)	1.52(0.14)
S+O	10.58(0.55)	11.10(0.45)	10.48(0.37)	12.26(3.30)	14.13(4.83)
Ash	5.89(0.55)	10.78(0.69)	9.11(1.32)	24.39(18.9)	32.50(29.6)

* Numbers in parentheses represent one standard deviation.

<d> = Arithmetic average of particle range in microns

TABLE Ib

ELEMENTAL COMPOSITION OF PARENT, DELIVERED AND RESIDUAL PARTICLES:
PSOC 1451D, 20 - 30 MICRON PARTICLES

SAMPLE	%C	%H	%N	%S+O	%ASH*
PARENT-1	75.19	4.94	1.48	9.66	8.69
PARENT-2	75.25	4.95	1.45	9.52	8.80
PARENT-3	75.00	4.91	1.45	9.82	8.80
PARENT-4	75.06	4.90	1.45	9.78	8.80
DELIVERED-1	78.49	5.08	1.53	10.08	4.80
DELIVERED-2	78.54	5.08	1.50	10.36	4.50
DELIVERED-3	78.56	5.12	1.51	10.09	4.69
DELIVERED-4	78.59	5.08	1.48	10.01	4.80
RESIDUAL-1	74.46	4.91	1.41	9.49	9.69
RESIDUAL-2	74.42	4.89	1.43	9.84	9.39
RESIDUAL-3	74.45	4.90	1.45	9.99	9.19
RESIDUAL-4	74.44	4.91	1.45	9.78	9.39

TABLE II
TAR YIELDS AND MOLECULAR WEIGHTS

REACTOR/ PARAMETERS	PARTICLE SIZE [m]	ATM.	POWER DENSITY [W/CM ²]	Mn	Mw	% TAR YIELD	RUN I.D.
HG 450/2 *	49	VAC	0.62	626	839	14.2	229B
HG 550/2	49	AR	0.74	510	703	14.9	238A
HG 600/10	49	VAC	0.88	594	775	25.1	239A
HG 550/2	49	VAC	0.94	664	960	35.3	232C
HG 600/10	49	HE	1.3	522	692	12.7	242A
HG 350/1	49	VAC	1.8	655	948	20.0	224B
HG 800/2.5	49	VAC	1.9	621	855	21.0	221A
HG 800/2.5	49	VAC	1.9	610	843	24.4	237B
HG 800/2.5	254	VAC	2.0	639	869	25.1	246A
HG 800/2.5	127	VAC	2.1	616	841	28.4	245A
HG 800/2	774	VAC	2.3	616	875	24.3	253A
HG 800/2.5	774	VAC	2.3	632	869	23.3	247A
HG 800/2.5	49	AR	2.3	520	734	17.5	235C
EF 900/3 **	64	N2	50.0	485	698	****	017
EF 900/9	64	N2	-	490	709	-	018
EF 900/22	64	N2	-	382	560	-	019
EF 1000/3	64	N2	80.0	531	766	****	020
EF 1000/9	64	N2	-	406	596	-	021
EF 1000/22	64	N2	-	275	407	-	022
FL 1.8/30 ***	49	HE	225(32)	686	1059	6.0	705J
FL 1.5/60	49	HE	285(40)	784	1184	12.0	703C
FL 1.5/90	49	HE	430(60)	699	1134	19.0	704B
FL 2.2/60	49	HE	730(96)	545	898	17.0	706E
FL 1.8/30	49	AR	225(122)	714	1121	19.0	707C
FL 1.8/30	49	VAC	225	764	1180	23.0	709B
FL 1.5/60	49	VAC	285	663	1054	28.4	713B
FL 2.2/60	49	AR	729(293)	630	955	22.0	708B

Footnotes:

- * HG X/Y - heated grid with 1000 C/sec ramp to X C, hold for Y sec, then 1000^o C/sec ramp to 800^o C, hold for 2.5-Y sec. The 600/10 runs are an exception: ramp to 600^o C and hold for 10 sec.
- ** EF X/Y - entrained flow with X C gas temperature and Y" sampling position 900^o C: 3"- 40 msec; 9" - 110 msec; 22" - 250 msec
1000^o C: 3"- 40 msec; 9" - 100 msec; 22" - 230 msec
- *** FL X/Y - flash lamp with X KV capacitor bank voltage and Y% neutral density filter. Values are time-averaged delivered irradiance; values inside parentheses are time-averaged net power density calculated from heat balance considerations. See Table III for characteristics of flash pulses.
- ***** - Not measured directly; at 3" residence time is estimated be about 20% (daf) of the parent coal mass from heated grid and flash lamp investigations. This yield represents the major fraction of the total volatile yields (Ref. 25) in 40 msec.

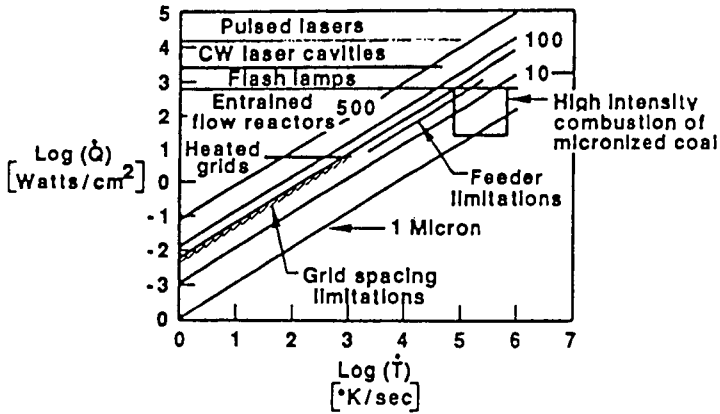
TABLE III
COMPARISON OF MOLECULAR WEIGHTS OF COAL DERIVED COMPOUNDS

SAMPLE	TECHNIQUE	Mn	Mw	MWD RANGE	INVESTIGATOR(S)
Pitt #8	SEC THF				this work
1 atm HG tar		500-525	675-750	100-3500	
vac HG tar		575-675	775-975	100-3500	
EF tar		275-550	400-775	100-3500	
1 atm FL tar		550-800	900-1200	100-5000	
vac FL tar		650-775	1050-1200	100-5000	
Pitt #8	SEC/VPO pyridine				Oh (1985)
HG tars:					
1 atm		350	-	100-1200	
vac		400	-	100-1200	
HG char extracts:					
1 atm		450	-	100-1500	
vac		500	-	100-1500	
Pitt Bruceton	SEC/VPO THF				Unger & Suuberg (1984)
HG tars:					
1 atm		500-700	-	100-4000	
vac		750-900	-	100-4000	
HG 1 atm char extracts:		750-1000	-	100-4000+	
Pitt #8 CO2 laser	SEC				Ballantyne et al. (1983)
1 atm tar	THF	223?	394?	60-3000	
Low Beam Shaw 84.2% C 115°C pyridine raw coal extract	Ebullio- scopy pyridine	870	-	-	Dormans & van Krevelen (1960)

REFERENCES

1. Freihaut, J.D., Zabielski, M.F. and Seery, D.J., Nineteenth Symposium (Int'l.) on Combustion, The Combustion Institute, 1159 (1982).
2. Freihaut, J.D. and Seery, D.J., ACS Div. of Fuel Chem., Preprints, 27, No. 2, 89 (1982).
3. Howard, J.B. in Chemistry of Coal Utilization, Sec. Supp. Vol. (ed. by Elliott, M.A.), John Wiley and Sons, New York, 340ff (1981).
4. Fong, W.S., Khalil, Y.F., Peters, W.A. and Howard, J.B., Fuel, 65, 195 (1986).
5. Suuberg, E.M., et al., Seventeenth Symposium (Int'l.) on Combustion, The Combustion Institute, Pittsburgh, 117 (1979).
6. Freihaut, J.D. and Seery, D.J., Proceedings of the International Conference on Coal Science, IEA, 957 (1985).
7. Freihaut, J. D., Proscia, W. M. and Seery, D. J. Proceedings of the Third Annual Pittsburgh Coal Conference, 684 (1986).
8. Unger, P.E., and Suuberg, E.M., Fuel, 63, 606 (1984).
9. Oh, M.S., Ph.D. Thesis, M.I.T., Cambridge, MA, 1985.
10. Solomon, P.R., Squire, K.R., and Carangelo, R.M., Proceedings of the International Conference on Coal Science, IEA, 945 (1985).
11. Kaiser, M., Wanzl, W., van Heek, K.H. and Juntgen, H., Proceedings of the International Conference on Coal Science, IEA, 899 (1985).
12. Cotter, R.J., Analytical Chemistry, 52, No. 14, 1589A.
13. Van der Peyl, G.J.Q., Haverkamp, J. and Kistemaker, P.G., Internat. Jnl. of Mass Spectrometry and Ion Physics, 42, 125 (1982).
14. Beuhler, R.J., Flanigan, E., Greene, L.J. and Friedman, L., J. Amer. Chem. Society, 96, No. 12, 3990 (1974).
15. Heresch, F., Schmid, E.R. and Huber, J.F.K., Anal. Chem., 52, 1803 (1980).
16. Posthumus, M.A., Kistemaker, P.G. and Meuzelaar, H.L.C., Analytical Chemistry, 50, No. 7, 985 (1978).
17. Cotter, R.J., Analytical Chemistry, 52, 1770 (1980).
18. Stoll, R. and Rollgen, F.W., Org. Mass. Spec., 14, No. 12, (642) (1979).
19. Kistemaker, P.G., Lens, M.M.J., Van der Peyl, G.J.Q., and Boerboon, A.J.H., Adv. in Mass Spectrometry, 8A, 928 (1980).

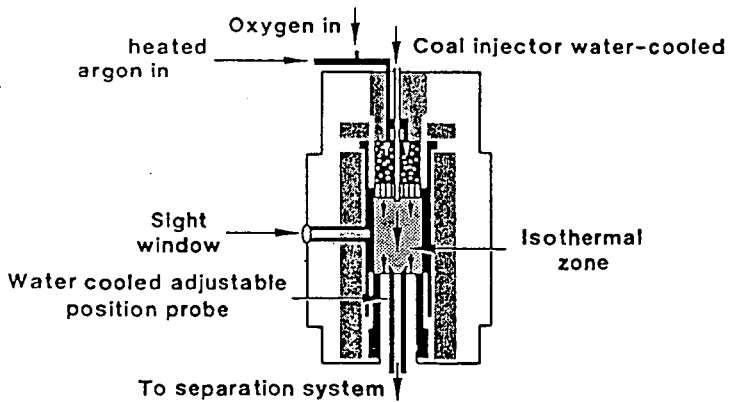
Fig. 1 Reactor Heat Transfer Regimes



841147L41

FIGURE 2

ENTRAINED FLOW REACTOR FOR COAL DEVOLATILIZATION



841147L51

FIGURE 3

AEROSOL - CHAR SEPARATION APPARATUS

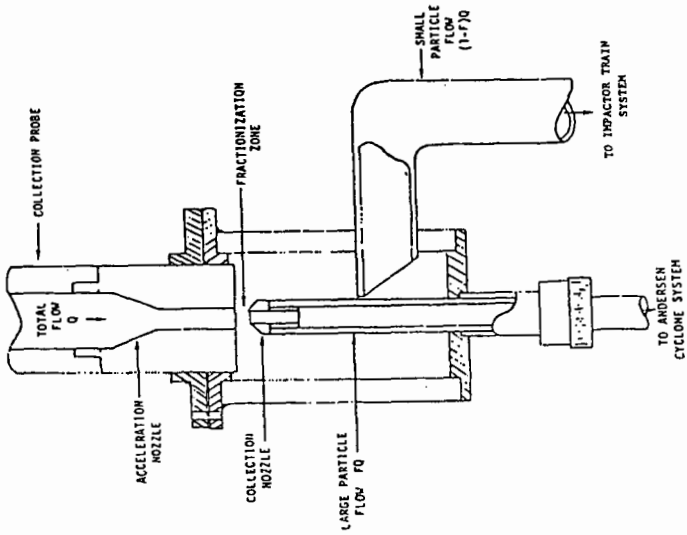


FIGURE 4

SAMPLE COLLECTION SYSTEM

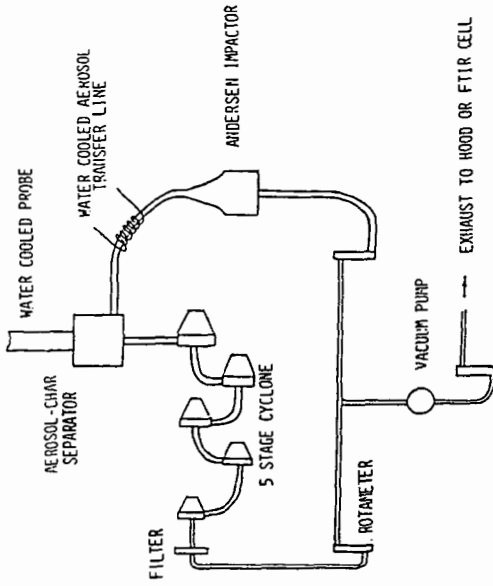


FIG. 5

EFFECT OF PRESSURE On tar molecular weight distributions

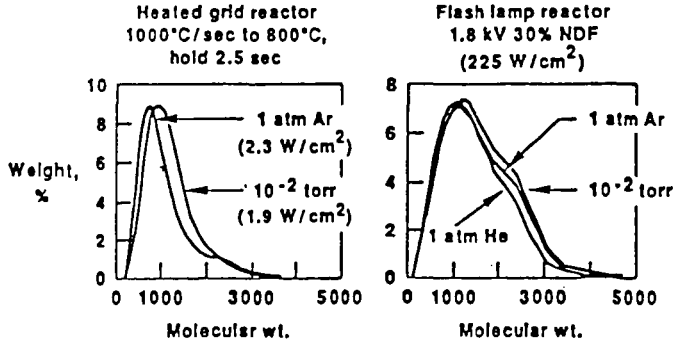
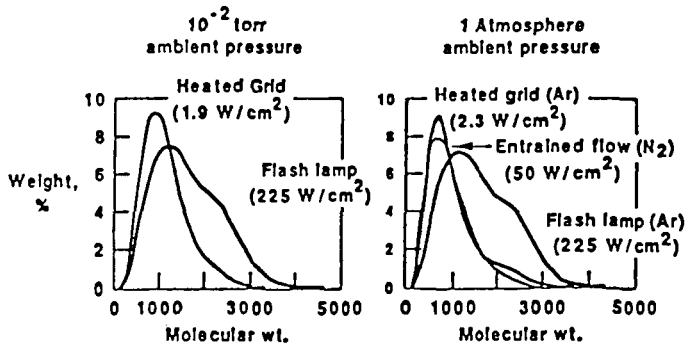


FIG. 6

EFFECT OF DIFFERENT REACTORS On tar molecular weight distributions



Pyrolysis of Coal at High Temperatures

Peter F. Nelson, Ian W. Smith and Ralph J. Tyler

CSIRO Division of Fossil Fuels, PO Box 136, North Ryde 2113, Australia

Introduction

Pyrolysis of coal at high heating rates is the initial step in its utilization by combustion, gasification or liquefaction. This involves the thermal decomposition of the coal's organic structure and the release of volatile products, which may account for up to 70% weight loss of the coal. Knowledge of the behaviour of the many volatile species liberated during pyrolysis is warranted, since their composition, rate of release and secondary reactions will have an important influence on such practical considerations as ignition, rate of combustion and trace gaseous and particulate emissions.

For many coals the condensed volatile species, or tar, comprise a major part of the volatile yield in coal devolatilization(1). They have been suggested as an important source of soot during coal combustion(2,3), and they have potential as models of coal structure. Thus an understanding of secondary reactions of tars is necessary for a complete model of coal devolatilization to be developed. The tars can crack to form soot, char and gases. Secondary reactions of the char involving ring condensation and gas evolution (mainly CO and H₂) will influence reactivity of the char towards gasification or combustion.

This paper presents data on the pyrolysis of a subbituminous coal and of tar produced by the rapid pyrolysis of this coal in a small fluidised bed reactor and in a shock tube. Kinetic parameters for light gas formation from secondary reactions of the tar have been determined. The results also provide evidence that secondary reactions of the tar are a source of polycyclic aromatic hydrocarbons (PAH) observed during pyrolysis. Data are also presented to show the effect of preparation conditions on the combustion kinetics of chars produced by rapid pyrolysis.

Experimental

The design and operation of the fluidised bed pyrolyzer has been described previously(1,4,5), as has the shock tube used for the high temperature cracking (6,7). Light gases were analyzed by gas chromatography. Tar components were recovered from the fluidised bed pyrolyzer by filtration through a Soxhlet thimble held at liquid nitrogen temperature, extracted with dichloromethane and analyzed by high resolution gas chromatography(5). Millerran subbituminous coal was used for all experiments (analysis wt%; C, 79.1; H, 6.5; N, 1.2; S, 0.6; O (diff.), 12.6).

Chars for the combustion studies were prepared, using a large-scale fluidised bed pyrolyser at temperatures of 540, 600 and 800°C. The product char was separated hot from the pyrolyser product gas, cooled, sampled, and then sieved to give size-graded fractions. The combustion reactivity of the char was determined using a flow reactor, and an ignition apparatus(10). The char samples contained appreciable amounts of volatile matter, the 600°C material having a standard VM yield of 16.6% (daf), and a hydrogen content of 4.0%.

Results

Kinetic parameters for secondary cracking of tar

Pyrolysis reactions of the coal under rapid heating conditions were separated from decomposition reactions of the tar to allow the vapour phase cracking reactions to be investigated free from influences of the original coal or char. This was

achieved by linking a fluidised bed pyrolyzer, operating at a low temperature (600°C) to minimise secondary reactions, to a shock tube capable of providing temperatures up to 2000K and residence times of 1-2 ms.

Arrhenius parameters for the rates of formation of CH_4 , C_2H_2 , C_2H_4 , C_3H_6 , C_6H_6 and CO were determined and are presented in Table 1. Rates of production of C_2H_4 and C_3H_6 yielded activation energies of 230 and 260 kJ mol^{-1} respectively and are thus in excellent agreement with typical Arrhenius parameters obtained for the pyrolysis of long chain gaseous hydrocarbons(11,12). Thus the likely precursors of these alkenes are long chain n-alkyl groups. Recent studies(13) have shown that Millmerran flash pyrolysis tar contains at least 23 wt% n-alkyl groups of which about 40% are present as free alkanes and alkenes and the balance are bound to other structures, probably as substituted aromatics. Yields of C_2H_4 and C_3H_6 observed from the tar cracking are in excellent agreement with this n-alkyl content.

Kinetics for the lumped disappearance of long chain alkanes and alkenes have also been determined for pyrolysis in the fluid bed reactor. These results are presented in Fig. 1 and give an activation energy of 237 kJ mol^{-1} in good agreement with literature values for the decomposition of n-octane(11) and n-hexadecane(12).

Activation energies for the formation of CH_4 , C_6H_6 and CO from the tar cracking are low and in the range 110 - 140 kJ mol^{-1} . This implies that many different functional groups in the tar contribute to the formation of these species with very different rates leading to a low apparent activation energy.

Formation of Polycyclic Aromatic Hydrocarbons (PAH)

Tar reactions have been identified as a source of the soot produced in both pyrolysis and combustion systems(2,3). Recent results(5) have also shown that the predominant components of the tar produced at temperatures greater than 800°C in the fluid bed reactor are PAH with up to five rings.

Mechanisms postulated for the formation of PAH in the combustion of simple hydrocarbons in flames include both ionic(14) and free radical(15) processes. The species observed, and which are regarded as important intermediates in the formation of the larger aromatic species, include phenylacetylene, styrene, indene, naphthalene and acenaphthalene. The free radical mechanisms involve addition reactions of aromatic radicals (predominantly benzyl and phenyl) to unsaturated aliphatics such as acetylenic species and stabilisation of the adduct by the formation of six-membered rings. Recently Homann(16) has shown that these species occur in approximately equivalent relative amounts in flames burning a very wide variety of fuels.

The predominant species produced from coal pyrolysis at high temperatures where tar cracking is important are remarkably similar to those found in the flame studies. Fig. 2 shows yields of phenylacetylene, styrene and indene obtained from the pyrolysis of Millmerran coal in the fluid bed reactor. Analysis of the tar by FTIR shows that acetylenic species have also undergone addition reactions with the larger aromatic species.

The similarity of the species distribution observed for the coal pyrolysis products and the flame products strongly suggests that a common mechanism is responsible for the formation of PAH in these two systems. Thus in addition to their importance for soot formation, secondary reactions of volatiles are an important source of PAH formed in combustion.

Char reactivity

The combustion reactivity of the three chars determined in the flow reactor (production temperatures 540, 600 and 800°C respectively) is given in Fig. 3(a). At a

combustion temperature of $\sim 700^{\circ}\text{C}$ the reactivities of the chars show an inverse relationship to their preparation temperature the lower the preparation temperature the higher the reactivity(17). At 1000°C these differences have largely disappeared.

The question then arises as to the relative contributions to the observed reactivity by the consumption of the volatile and solid components of the char. The data in Fig. 3(a) were determined using a flow reactor when the particles and hot gas were mixed some distance before the burning suspension passed the positions in the reactor where rate measurements were made. There is some indication(17) that the volatile matter is evolved rapidly, and that the burning rate data are for the consumption of the solid char after the volatiles have been released.

Support for this view is given by Rybak *et al.*(10) where the reactivity of the 600°C char was determined from a measurement of particle ignition temperature. It was found that the ignition temperature was affected by the volatile content of the char - the more times the char was cycled through the heated ignition reactor (in the absence of oxygen), the higher the ignition temperature ultimately measured. Fig. 3(b) shows that the reactivity of the char reduces with increasing heating time (increasing number of cycles through the reactor) in a manner similar in reactivity to the reactivity change with pyrolysis temperature shown in Fig. 3(a). After eight cycles the reactivity is close to that measured in the flow reactor (and in a quite different reactor at the Sandia Laboratories(18)).

References

1. Tyler, R.J. Fuel 1980, 59, 218
2. Seeker, W.R., Samuelsen, G.S., Heap, M.P. and Trolinger, J.D. Eighteenth Symposium (International) on Combustion, p.1213, The Combustion Institute, 1981.
3. McLean, W.J., Hardesty, D.R. and Pohl, J.H. Eighteenth Symposium (International) on Combustion, p.1239, The Combustion Institute, 1981.
4. Tyler, R.J. Fuel 1979, 58, 680.
5. Nelson, P.F. and Tyler, R.J. Twenty-first Symposium (International) on Combustion, in press, 1987
6. Doolan, K.R., Mackie, J.C. and Weiss, R.G. Combust. Flame 1983, 49, 221.
7. Doolan, K.R., Mackie, J.C. and Tyler, R.J. Fuel 1987, 66, 572.
8. Edwards, J.H. and Smith, I.W. Fuel, 59, 674-680, 1980.
9. Mulcahy, M.F.R. and Smith I.W., Proc. Conf. CHEMECA 70, Session 2, pp101-118, Butterworths, 1970.
10. Rybak, W., Zembruski, M. and Smith, I.W., 21st Symposium (International) on Combustion, 1986 (in press).
11. Doolan, K.R. and Mackie, J.C. Combust. Flame 1983, 50, 29.
12. Rebeck, C. in Pyrolysis, Theory and Industrial Practice (L.F. Albright, B.L. Cryres and W.H. Corcoran, Eds) p.69, Academic, 1983.
13. Nelson, P.F. Fuel, in press
14. Hayhurst, A.N. and Jones, H.R.N. J. Chem. Soc. Faraday Trans. 2, 1987, 83, 1.
15. Bittner, J.D. and Howard, J.B. Eighteenth Symposium (International) on Combustion, p.1105, The Combustion Institute, 1981.
16. Homann, K.H. Twentieth Symposium (International) on Combustion, p.857, The Combustion Institute, 1985.
17. Young, B.C. Proc. Int. Conf. on Coal Science, p.260, Dusseldorf, 1981.
18. Mitchell, R.E. and McLean, W.J. 19th Symposium (International) on Combustion, p.1113, The Combustion Institute, 1982.

Table 1 Kinetic parameters for formation of products from tar cracking in the shock tube.

Species Formed	A/s ⁻¹	E _a /kJ mol ⁻¹
CH ₄	7 x 10 ⁶	110
C ₂ H ₂	5 x 10 ⁹	220
C ₂ H ₄	2 x 10 ¹²	230
C ₃ H ₆	5 x 10 ¹³	260
C ₆ H ₆	7 x 10 ⁶	110
CO	2 x 10 ⁸	140

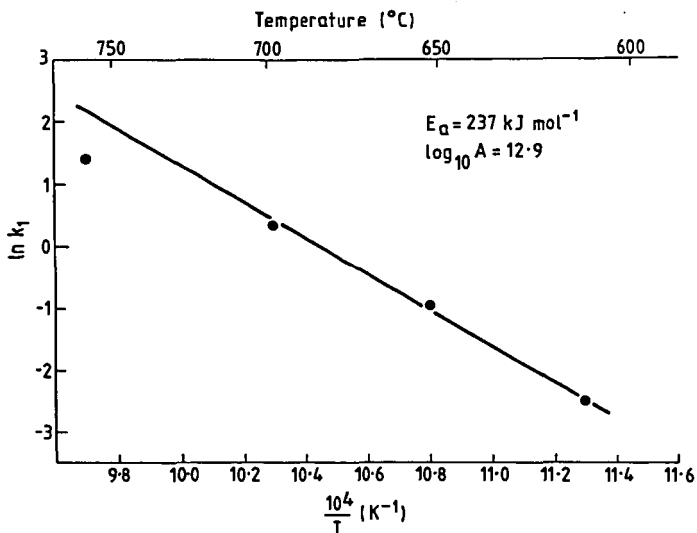


Fig. 1 Arrhenius relationship for polymethylene disappearance in fluidised bed reactor.

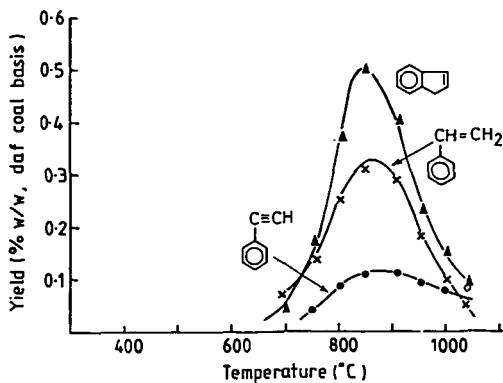


Fig. 2 Yields of indene, styrene and phenylacetylene as a function of temperature for pyrolysis of Millmerran coal.

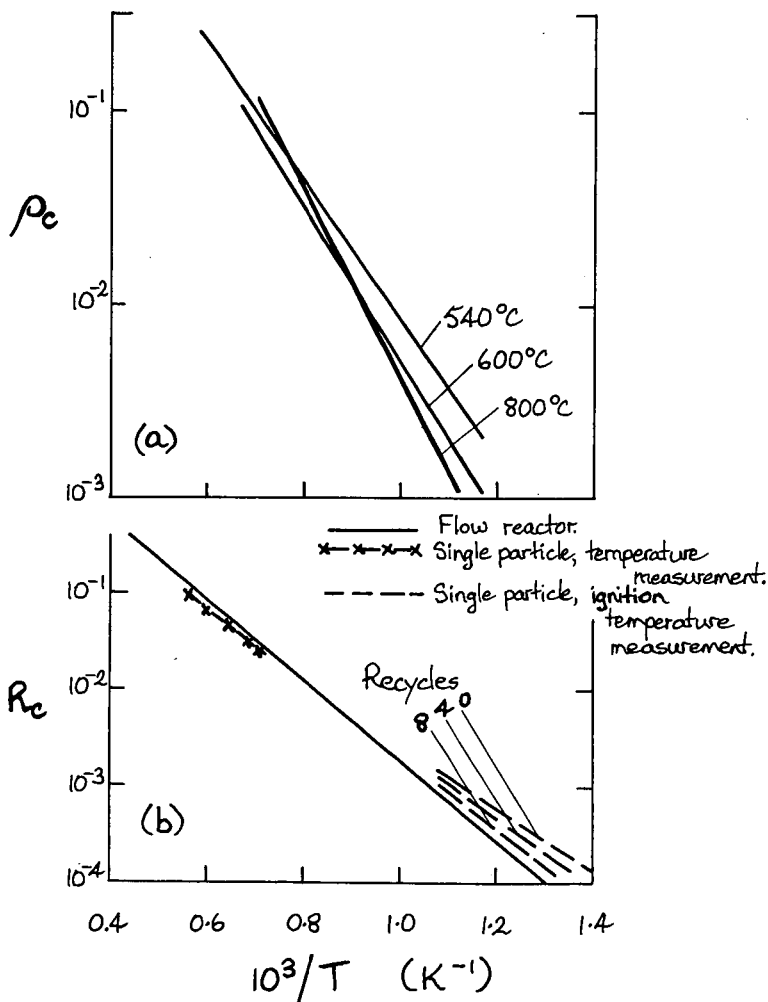


Fig.3. Reactivity of Sub-bituminous Coal Char: (a) as a function of pyrolysis temperature; (b) by various techniques, showing effect of heating time.

LOW TEMPERATURE ISOTHERMAL PYROLYSIS OF ILLINOIS NO. 6 AND WYODAK COAL

Francis P. Miknis, T. Fred Turner, and Lonny W. Ennen

Western Research Institute
Box 3395, University Station
Laramie, Wyoming 82071

INTRODUCTION

Despite what appear to be sufficient supplies of petroleum and natural gas to meet current U.S. energy needs, it is almost certain that future U.S. energy demands will be met in part by synthetic fuels produced from solid fossil fuels. The vast U.S. reserves of coal, in particular, have and will continue to receive considerable attention as a source of synthetic fuels. There are, however, certain fundamental constraints that limit the efficient processing and conversion of coal to synthetic fuels. Besides their chemical and physical heterogeneity, coals have highly aromatic chemical compositions. The high carbon aromaticity means that coals are hydrogen-deficient and as such do not readily convert to liquid and gaseous products. Consequently, innovative approaches are required to efficiently convert these hydrogen deficient materials to useful synthetic fuels.

Most coal conversion processes require thermal processing; therefore, pyrolysis is an important initial step in all coal utilization and conversion processes. Although coal pyrolysis has been studied extensively for several decades (1-4) it continues to be an active area of coal research. In part, this is a result of coal researchers' awareness of the need to understand pyrolysis in relationship to the basic structure of coal.

As a first step towards a systematic approach to understanding the relationship between coal structure and its conversion during pyrolysis, isothermal decomposition studies in the temperature range of 375°C to 425°C have been conducted on Illinois No. 6 and Wyodak coals. While prevailing attitudes favor the use of nonisothermal techniques to study coal pyrolysis, these techniques do not easily allow direct measurement of all the reaction products. Consequently, detailed chemical analyses of the reaction products are usually absent in such studies. In particular, intermediate states such as the metaplast are seldom measured directly.

With isothermal methods, it is possible to measure all the products of thermal decomposition including soluble intermediates. In addition to obtaining the overall weight conversions to products, detailed chemical and spectroscopic analyses can be obtained for each product class. For example, elemental analyses of all the products provide detailed carbon, hydrogen, sulfur, nitrogen, and oxygen balances. Solid and liquid state ^{13}C NMR measurements can be used to determine the partitioning of aliphatic and aromatic carbon in the products.

EXPERIMENTAL

Coal Samples

Isothermal pyrolysis experiments were conducted on Illinois No. 6 high volatile bituminous and on Wyodak subbituminous coal samples. Both coals were crushed and screened to obtain a 20/45 mesh particle size distribution. The initial crushed sample was thoroughly mixed and successively riffled to obtain aliquots of approximately 22 grams. Pyrolysis studies were conducted on samples taken from these aliquots. Ultimate and proximate analyses and carbon aromaticities of the two coals are given in Table 1.

Table 1. Analyses of Coal Samples

	Illinois No. 6	Wyodak
Proximate (% mf)		
Ash	8.1	8.0
Volatile Matter	39.0	47.0
Fixed Carbon	52.9	45.0
Ultimate (% mf)		
Hydrogen	5.3	5.5
Carbon	74.0	67.5
Nitrogen	1.0	0.8
Sulfur	3.4	0.7
Oxygen (diff)	8.3	17.5
Ash	8.1	8.0
Carbon Aromaticity	0.673	0.657

Pyrolysis Reactor System

The isothermal pyrolysis studies were carried out in a heated sand-bath reactor system described in detail elsewhere (5). In this system, nominally 10- to 20-gram samples were heated to reaction temperature by quickly immersing a tube reactor containing the coal sample into a preheated fluidized sand-bath. Typically, the coal sample reached the predetermined reaction temperature in less than 2 minutes. The reaction was quenched by removing the reactor from the sand bath and spraying liquid CO₂ on its surface. A helium sweep gas flow rate of 30 cc/min was used to remove the products from the reaction zone. The liquid product was collected in a dry-ice trap. Gaseous products were analyzed by gas chromatography, either by collecting the total gaseous product in an evacuated vessel or by analyzing the product gas on-line.

Material balances were calculated by measuring the weight change of the coal sample, the weight of collected liquid, the volume of collected water, and the weight of each gas component. The gas evolution curves were integrated, taking into account analytical system delays and backmixing, to calculate the total amount of gas evolved during each experiment. The reactor material balance closures were typically 100.2 ± 0.7%.

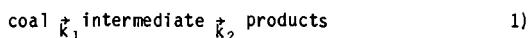
Product Analyses

Elemental analyses (CHN and S) were obtained on the solid and liquid reaction products using standard instrumental techniques. Molecular weights were determined by vapor phase osmometry, using pyridine or methylene chloride as a solvent. Liquid state ¹³C NMR measurements were made on a Varian CFT-20 or a JEOL 270 MHz NMR spectrometer. Solid state ¹³C NMR measurements of the solid products were obtained at the NSF Regional NMR Center at Colorado State University. Gas analyses were obtained on a Hewlett Packard 5830 gas chromatograph modified to obtain complete gas analyses as frequently as every 3 minutes.

RESULTS AND DISCUSSION

Soluble Intermediate

One objective of this work was to investigate the transient nature of intermediate products that are formed during pyrolysis. Generally, global models of coal pyrolysis involve some form of intermediate (6-9). The simplest of these models can be written (9),



The intermediate is often referred to as "thermobitumen" (10) or "metaplast" (6). Thermobitumen is the primary tar or bitumen formed during the initial stages of pyrolysis and acts as a plasticizer for the coal. Metaplast refers to coal which has been transformed into a fluid mass via depolymerization reactions, i.e., a metastable, plastic state. Neither material is defined in terms of solubility in a given solvent as, for example, the term bitumen is in oil shale pyrolysis. In fact, van Krevelen et al. (11) preferred the term metaplast to avoid the connotation that thermobitumen is a completely soluble material in a common petroleum solvent. Nevertheless, the properties and kinetic behavior of the soluble portion of the intermediate are known to affect the plasticity and conversion behavior of coals (12,13).

In this work, the residue coal from each isothermal pyrolysis experiment was extracted with chloroform to obtain information about the chloroform soluble portion of the intermediate. Chloroform was chosen over other commonly used solvents, such as pyridine, because it does not appreciably dissolve the raw coal and gives fairly high yields of soluble products from pyrolyzed caking coals (12).

Only small amounts of material were extractable with chloroform at any stage of pyrolysis for either coal (Figures 1 and 2). In the context of the simple model (Equation 1), the data in Figures 1 and 2 illustrate that either 1) $k_2 \gg k_1$, and the soluble material is not retained long enough to plasticize the coal or 2) significant devolatilization occurs directly from the raw coal, without involving an intermediate state. The latter has been suggested to account for the increase in volatile matter with pyrolysis temperature, as well as development of fluidity in coal (9). We have observed a similar behavior of soluble intermediates during isothermal pyrolysis of New Albany shale from Kentucky, and have concluded that the greater the carbon aromaticity of the source material, the greater is the direct conversion of source material to products (primarily residue) (14).

Properties of Residue Products

Global models of coal pyrolysis, such as that depicted by Equation 1, do not incorporate any components of coal structure, although the ultimate yields of pyrolysis products are determined to a large degree by the carbon structure of the raw coal. With isothermal pyrolysis methods and solid state ^{13}C NMR techniques, it is now possible to measure changes that occur in the carbon structure of coal as a function of time and temperature. In addition, by obtaining the ultimate and proximate analyses of the residue coals, it is possible to monitor these changes quantitatively on a mass basis. These data were collected during the 425°C experiments for Wyodak and Illinois No. 6 coals (Figure 3).

The data in Figure 3 confirm that the aliphatic carbon weight loss behavior is similar to that of the total carbon. Conversely, the aromatic carbon remains relatively constant with time. Chou et al. (15) have observed a similar behavior of chars produced from flash pyrolysis of Illinois No. 5 coal at charring temperatures from 300°C to 800°C. These data support the theory that coal devolatilization

involves primarily the breaking of aliphatic carbon bonds and that the aromatic carbon tends to remain in the residue (16).

Total Aromatic Carbon in Products

During pyrolysis of fossil fuels, a net increase always occurs in the amount of aromatic carbon in the products (tar plus residue) over that in the starting material. This increase results from aromatization reactions of aliphatic moieties and the associated release of light, high hydrogen-content aliphatic species. Aromatization of hydroaromatic structures, such as tetralin, is a likely mechanism for contributing to the increase in aromatic carbon.

The extent of aromatization during pyrolysis can be determined by combining solid and liquid ^{13}C NMR measurements and the carbon mass balance data (Figures 4 and 5). For some experiments NMR carbon aromaticity and/or total organic carbon measurements were not obtained because insufficient quantities of tars were produced. In these cases the amount of aromatic carbon in the tar was estimated using the weight percent of produced tar and the average values of organic carbon and/or carbon aromaticities from other experiments at the same temperature. These data are denoted by the symbol θ (Figures 4 and 5). The increases in aromatic carbon content for the Illinois No. 6 and Wyodak coals are about 18% and 10%. The reason for the low values is that only about 10% of the raw coals was converted to tars at the longest time (480 min) and highest temperature (425°C) studied.

An interesting feature of the data is that the net production of aromatic carbon approaches its limiting value during the early stages of pyrolysis (Figures 4 and 5). For example, at 425°C the net production of aromatic carbon for the Illinois No. 6 coal has reached 95% of the limiting value within 2 minutes (Figure 4c). Similar behavior is noted for the Wyodak coal. Thus, aromatization of the aliphatic moieties appears to be a very facile chemical reaction; however, it is not possible from these data to determine to what extent these reactions occur directly in the solid coal or in the produced tars.

ACKNOWLEDGMENTS

The authors wish to acknowledge the Colorado State University Regional NMR Center, funded by NSF Grant No. CHE-8208821, for providing the solid state ^{13}C NMR data. This material was prepared with the support of the U.S. Department of Energy, Grant No. DE-FG22-85PC80531. However, any opinions, findings, conclusions, or recommendations expressed herein are those of the authors and do not necessarily reflect the views of DOE.

DISCLAIMER

Mention of specific brand names or models of equipment is for information only and does not imply endorsement of any particular brand.

REFERENCES

1. Anthony, D. B. and J. B. Howard. *AICHE Journal* 22, 625 (1976).
2. Howard, H. C. in Chemistry of Coal Utilization, (H.H. Lowry Ed.), John Wiley, New York, 1963, 340-394.
3. Howard, J. B. in Chemistry of Coal Utilization, 2nd Supplementary Volume (M.A. Elliot, Ed) Wiley-Interscience, New York 1981, 665-784.
4. Gavalas G. R. Coal Pyrolysis, Elsevier, New York, 1982.
5. Conn. P. J., H. J. Rollison, and F. P. Miknis. Laramie, Wy., October 1984, DOE Report, DDE/FE/60177-1791.
6. Chermin, H. A. G., and D. W. van Krevelen. *Fuel*, 36, 85 (1957).
7. Unger, P. E., and E. M. Suuberg. 18th Symposium (International) on Combustion, The Combustion Institute, Pittsburgh, PA, 1981, 1203-1211.
8. Schaub, G., W. A. Peters, and J. B. Howard. *AICHE Journal*, 31, 903 (1985).
9. Gaines, A. F. *Pure and Appl. Chem.*, 58, 833 (1986).
10. Berkowitz, N. An Introduction to Coal Technology, Academic Press, New York, 1979, p. 152.
11. van Krevelen, D. W., F. J. Huntjens, and H. N. M. Dormans. *Fuel*, 35, 462 (1956).
12. Dryden, I. G. C. and K. S. Pankhurst. *Fuel*, 34, 363 (1955).
13. Loison, R., Peytavy, A. F. Boyer, and R. Grillot, in Chemistry of Coal Utilization (H.H. Lowry, Ed) John Wiley, New York, 1963, 150-201.
14. Turner, T. F., F. P. Miknis, G. L. Berdan, and P. J. Conn, ACS Div. of Petrol. Chem. preprints, 32(1), 149 (1987).
15. Chou, M. M., D. R. Dickerson, D. R. McKay, and J. S. Frye. *Liq. Fuels Technol.*, 2, 375 (1984).
16. van Krevelen, D. W., and J. Schuyer. Coal Science, Elsevier, Amsterdam, 1957, p 191.

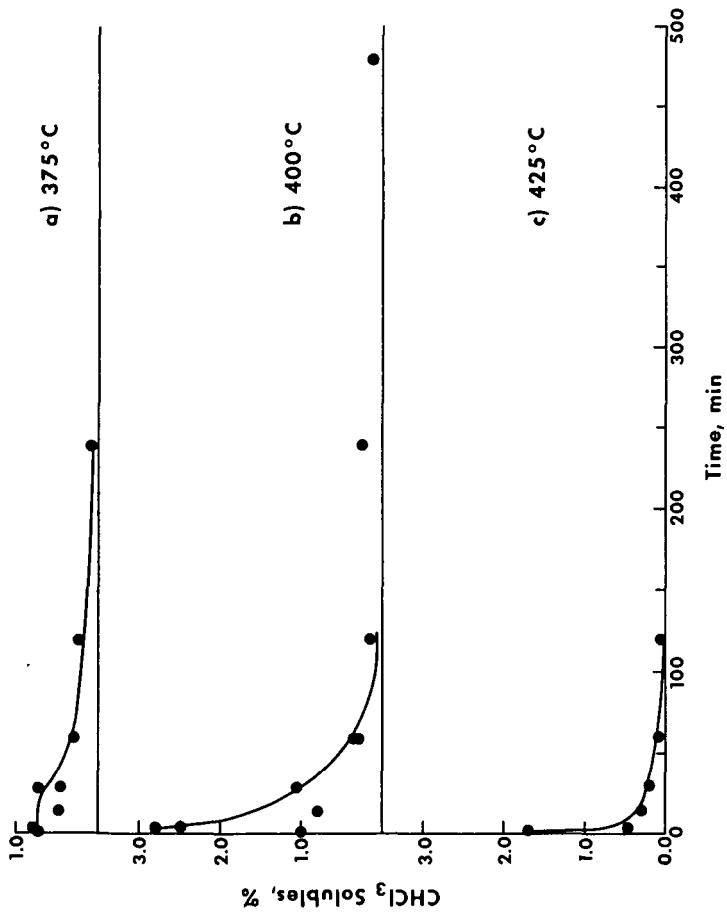


Figure 1. Chloroform-Extractable Material in Illinois No. 6 Coal vs. Time at a) 375°C, b) 400°C, and c) 425°C.

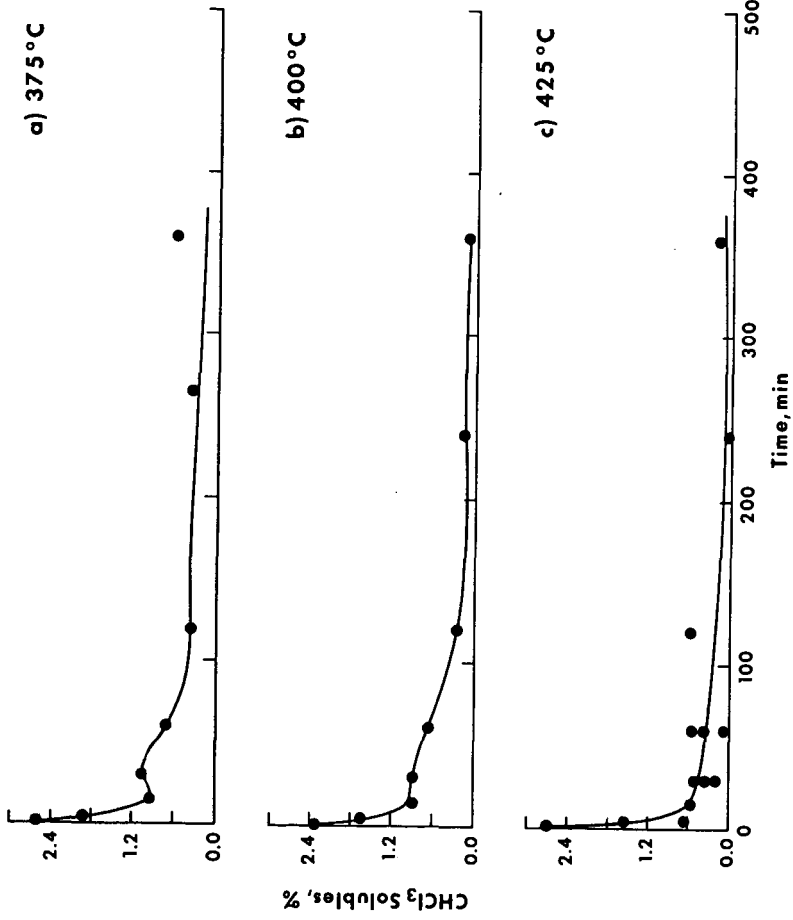


Figure 2. Chloroform-Extractable Material in Myodak Coal vs. Time at a) 375°C, b) 400°C, and c) 425°C.

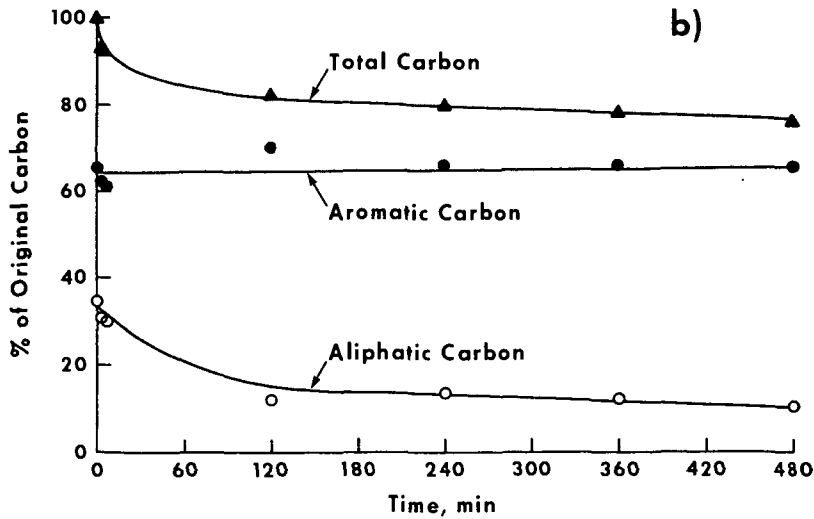
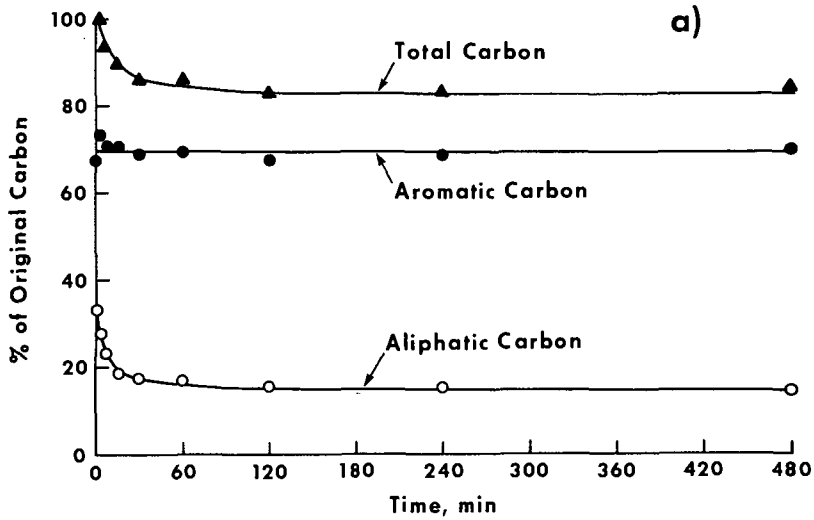


Figure 3. Distribution of Carbon Types vs. Time at 425°C for
 a) Illinois No. 6 and b) Wyodak Coal.

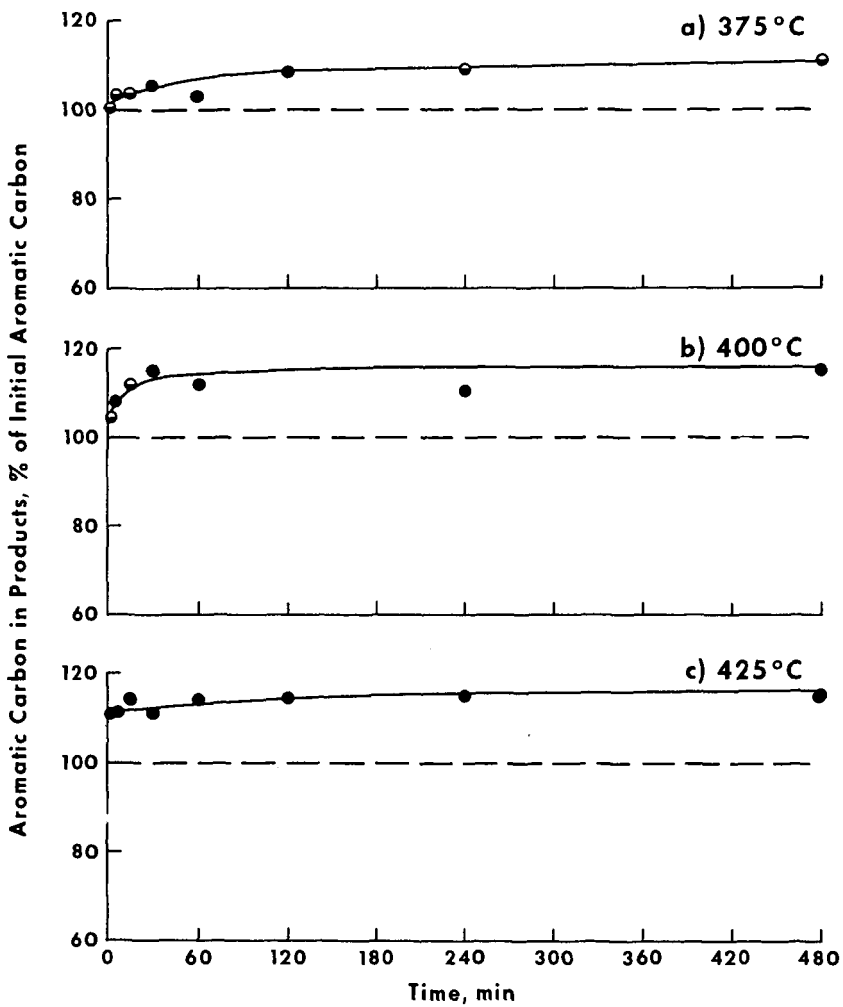


Figure 4. Total Aromatic Carbon in Products vs. Time for Illinois No. 6 Coal at a) 375°C, b) 400°C, and c) 425°C.

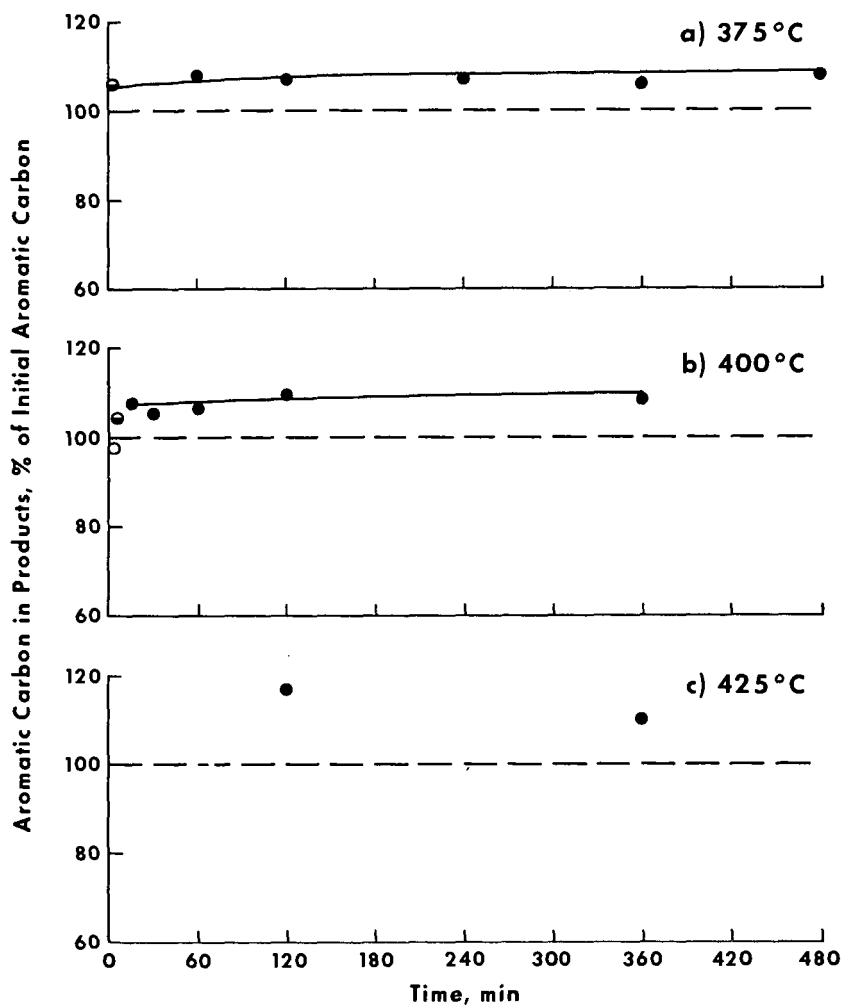


Figure 5. Total Aromatic Carbon in Products vs. Time for Myodak Coal at a) 375°C, b) 400°C, and c) 425°C.